

Third quantization of the electromagnetic field

J.D. Franson, Physics Dept., University of Maryland Baltimore County, Baltimore, MD 21250 U.S.A.

We consider an approach in which the usual wave function $\psi_j(x_j)$ in the quadrature representation of mode j of the electromagnetic field is quantized to produce a field operator $\hat{\psi}_j(x_j)$. Since the electromagnetic field is already second quantized, this corresponds to a third quantization. This approach allows certain calculations in quantum optics to be performed in a straightforward way in the Heisenberg picture. Aside from being a useful computational tool, this approach allows an interesting generalization of quantum optics and quantum electrodynamics that could be tested experimentally.

Particles cannot be created or destroyed in nonrelativistic quantum mechanics. Nevertheless, it is often useful to second-quantize the wave function $\psi(x)$ and its conjugate $\psi^*(x)$ to produce field operators $\hat{\psi}(x)$ and $\hat{\psi}^\dagger(x)$ that can formally annihilate or create particles at position x [1-7]. In this paper, a somewhat analogous approach is introduced in which the usual wave function $\psi_j(x_j)$ [8-12] in the quadrature representation of each mode j of the electromagnetic field is quantized to produce a field operator $\hat{\psi}_j(x_j)$. This approach allows certain calculations in quantum optics to be performed in a straightforward way in the Heisenberg picture, just as the use of second-quantized field operators is essential in solid-state physics, for example [13-17].

In quantum optics, each mode of the electromagnetic field is mathematically equivalent to a harmonic oscillator [8,11,18-20]. We can think of each of these harmonic oscillators as containing a single hypothetical particle whose excited states correspond to the presence of photons in the field, as illustrated in Fig. 1. As will be shown below, the operator $\hat{\psi}_j^\dagger(x_j)$ creates additional particles of that kind in the same harmonic oscillator potential as illustrated in Fig. 2. This generates a hyperspace of the usual Fock space. Since the electromagnetic field is already second quantized, this procedure corresponds to an additional or third quantization [21-26]. For lack of a better term, these hypothetical particles will be referred to as oscillatons [27-29].

The third-quantization approach is equivalent to conventional quantum optics and quantum electrodynamics if we use the standard Hamiltonian, which conserves the number of oscillatons. A more general theory that could be tested experimentally will also be described.

The second quantization of the normal modes of the classical electromagnetic field results in the usual harmonic oscillator raising and lowering operators \hat{a}_j^\dagger and \hat{a}_j that are responsible for the

creation and annihilation of photons [18-19]. The operators \hat{x}_j and \hat{p}_j can then be defined as

$$\begin{aligned}\hat{x}_j &= (\hat{a}_j + \hat{a}_j^\dagger) / \sqrt{2}, \\ \hat{p}_j &= -i(\hat{a}_j - \hat{a}_j^\dagger) / \sqrt{2}.\end{aligned}\quad (1)$$

The dimensionless operators \hat{x}_j and \hat{p}_j are referred to as the quadratures of the field in quantum optics [8-10,12], and they are proportional to the electric field of mode j and its time derivative. The quadratures can be directly measured using homodyne techniques [8-12,20,30] and they are used extensively to observe the nonclassical properties of squeezed states [8-11,20,31-32], for example.

For a pure state, the wave function $\psi_j(x_j)$ in the quadrature representation of a single mode j of the second-quantized electromagnetic field can be defined as usual [8-12] by

$$\psi_j(x_j) \equiv \langle x_j | \Psi_j \rangle. \quad (2)$$

Here $|x_j\rangle$ is an eigenstate of \hat{x}_j and $|\Psi_j\rangle$ is the state of mode j . For a single-mode field with a definite number n_j of photons (a Fock state), $\psi_j(x_j)$ corresponds to the usual energy eigenfunctions $\phi_n(x_j)$ of a harmonic oscillator that involve the Hermite polynomials [8].

The wave function $\psi_j(x_j)$ gives the probability amplitude that a homodyne measurement will result in that value of the x quadrature. It can be used in the Schrodinger picture to show that postselection based on homodyne measurements can violate Bell's inequality, for example [12,33]. The analysis of experiments of that kind (and others) can be done in the same way in the Heisenberg picture only if the operators $\hat{\psi}_j(x_j)$ and $\hat{\psi}_j^\dagger(x_j)$ are introduced. This can be of practical importance, since the

Heisenberg picture is often used to analyze quantum noise and decoherence in optical amplifiers [34-37], for example.

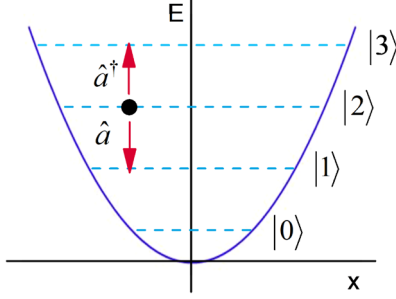


Fig. 1. A harmonic oscillator potential $U(x)$ (blue curve) in one dimension x that contains a single particle represented by a black dot. E is the energy of the particle and the energy eigenstates $|n\rangle$ are represented by dashed lines. The operators \hat{a}^\dagger and \hat{a} increase or decrease the energy of the particle by $\hbar\omega$. A single mode of the electromagnetic field is mathematically equivalent to a harmonic oscillator containing a single hypothetical particle whose excited states $|n\rangle$ correspond to n photons in the field [8,11,18-20].

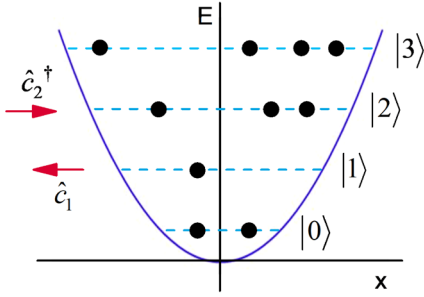


Fig. 2. A harmonic oscillator potential containing N identical bosons represented by black dots. The operators \hat{c}_n^\dagger and \hat{c}_n create or annihilate a particle in the oscillator potential in state $|n\rangle$. The field operator $\hat{\psi}^\dagger(x)$ creates a particle at coordinate x . In the case of the electromagnetic field, these hypothetical particles will be referred to as oscillatons.

Before the operators $\hat{\psi}_j(x_j)$ and $\hat{\psi}_j^\dagger(x_j)$ for the electromagnetic field are defined, it may be useful to briefly review the usual second-quantization formalism in nonrelativistic quantum mechanics. We will closely follow the text by Gordon Baym [1]. Consider a harmonic oscillator potential $U(x)$ in one dimension, as illustrated in Fig. 1. The eigenstates $|n\rangle$ of the Hamiltonian are represented by dashed lines. If there is only one particle in the potential, it can be represented by a single black dot occupying one of the

eigenstates as in Fig. 1. The usual raising and lowering operators \hat{a}^\dagger and \hat{a} increase or decrease the energy of the particle by one quanta, as indicated by the red arrows.

Even in nonrelativistic quantum mechanics, it is often convenient to introduce an operator \hat{c}_n^\dagger that formally adds or creates an additional particle in eigenstate $|n\rangle$ of the harmonic oscillator potential as illustrated by the red arrow in Fig. 2. Its adjoint \hat{c}_n annihilates a particle if one was there initially. If the particles are bosons, then it is possible to have more than one particle in eigenstate $|n\rangle$. N_n will denote the number of particles in eigenstate $|n\rangle$, and the total number of particles will be denoted by N with no subscript.

It will be assumed that the particles are identical bosons and that they satisfy the commutation relation

$$[\hat{c}_m, \hat{c}_n^\dagger] = \delta_{mn}. \quad (3)$$

The second-quantized field operator $\hat{\psi}(x)$ in the Schrodinger picture is then defined [1] as

$$\hat{\psi}(x) \equiv \sum_n \hat{c}_n \phi_n(x). \quad (4)$$

Here $\phi_n(x)$ is the eigenfunction corresponding to state $|n\rangle$. The fact that the $\phi_n(x)$ form a complete set of orthonormal functions can be combined with Eqs. (3) and (4) to show that

$$[\hat{\psi}(x), \hat{\psi}^\dagger(x')] = \delta(x-x'), \quad (5)$$

where $\delta(x-x')$ is the Dirac delta-function. This commutation relation can be used to derive the time dependence of the field operators in the Heisenberg picture.

So far, we have considered the second-quantization of an ordinary harmonic oscillator. The same approach will now be applied to each mode j of the electromagnetic field, which is mathematically equivalent to a harmonic oscillator containing a single hypothetical particle as in Fig. 1 [8,11,18-20]. The excited states $|n_j\rangle$ of the particle correspond to n_j photons in the field, and increasing its energy by $\hbar\omega_j$ corresponds to the addition of a photon.

As before, we introduce operators \hat{c}_{jn}^\dagger and \hat{c}_{jn} that create or annihilate particles in the harmonic

oscillator potential that represents mode j of the field, as in Fig. 2. The operator \hat{c}_{jn}^\dagger increases the number of particles in eigenstate $|n_j\rangle$ by one, which increases the dimensions of the usual Fock space to form a hyperspace. The particles will be assumed to be identical bosons, and the commutation relations of Eq. (3) can be used to show that

$$\begin{aligned}\hat{c}_{jn}|\dots, N_{jn}, \dots, N_{j0}\rangle &= \sqrt{N_{jn}}|\dots, (N_{jn}-1), \dots, N_{j0}\rangle, \\ \hat{c}_{jn}^\dagger|\dots, N_{jn}, \dots, N_{j0}\rangle &= \sqrt{N_{jn}+1}|\dots, (N_{jn}+1), \dots, N_{j0}\rangle.\end{aligned}\quad (6)$$

Here $|\dots, N_{jn}, \dots, N_{j0}\rangle$ denotes a state of the oscillator with N_{jn} particles in each of the eigenstates $|n_j\rangle$. This is a generalization of the usual Fock states $|n_j\rangle = |0, \dots, 1_{jn}, \dots, 0_{j0}\rangle$ that correspond to only one particle in the oscillator ($N_j = 1$).

It should be emphasized that these additional particles are not photons. For lack of a better term, we will refer to them as oscillatons. Increasing the energy of an oscillaton by $\hbar\omega_j$ corresponds to the addition of a photon. The excited states of the electromagnetic field with $N_j > 1$ will be referred to as hyperphotons. The indices j , n_j , and N_{jn} correspond to first, second, and third quantization, respectively, as is discussed in more detail in the supplemental information. The terms oscillaton [27-29], hyperphoton [38-40], and third quantization [21-26] have been used previously with different meanings.

New lowering and raising operators \hat{a}'_j and \hat{a}'_j^\dagger can be defined as

$$\begin{aligned}\hat{a}'_j &\equiv \sum_{n=1}^{\infty} \sqrt{n} \hat{c}_{j,n-1}^\dagger \hat{c}_{jn}, \\ \hat{a}'_j^\dagger &\equiv \sum_{n=0}^{\infty} \sqrt{n+1} \hat{c}_{j,n+1}^\dagger \hat{c}_{jn}.\end{aligned}\quad (7)$$

These operators reduce to the usual raising and lowering operators for $N_j = 1$. The vector potential $\hat{\mathbf{A}}(\mathbf{r})$ can be defined as usual [18] by

$$\hat{\mathbf{A}}(\mathbf{r}) = \sum_{j, \boldsymbol{\varepsilon}_j} \sqrt{\frac{2\pi\hbar c^2}{\omega_j L^3}} \left(\boldsymbol{\varepsilon}_j \hat{a}'_j e^{i\mathbf{k}_j \cdot \mathbf{r}} + \boldsymbol{\varepsilon}_j^* \hat{a}'_j^\dagger e^{-i\mathbf{k}_j \cdot \mathbf{r}} \right), \quad (8)$$

where L is the length used for periodic boundary conditions, $\boldsymbol{\varepsilon}_j$ are two orthogonal polarization

vectors, and c is the speed of light. A similar expression exists for the electric field.

In analogy with Eq. (4), the field operator $\hat{\psi}_j(x_j)$ for mode j of the electromagnetic field can now be defined in the Schrodinger picture as

$$\hat{\psi}_j(x_j) \equiv \sum_n \hat{c}_{jn} \phi_n(x_j). \quad (9)$$

The commutation relation $[\hat{\psi}_j(x_j), \hat{\psi}_j^\dagger(x_j')] = \delta(x_j - x_j')$ holds within each mode of the field as in Eq. (5). The field operator $\hat{\psi}_j(x_j)$ could be introduced in a more formal way by using the Lagrangian density and postulating the commutation relation of Eq. (5), but the approach presented here provides more insight.

Some of the useful properties of this approach will now be illustrated by calculating the loss and decoherence produced by a beam splitter in conventional quantum optics. Two free-space modes j and k of the electromagnetic field are assumed to be incident on a beam splitter as illustrated in Fig. 3. In the absence of any interaction between the two modes, the Hamiltonian \hat{H}_0 can be written in the form

$$\hat{H}_0 = \sum_{n_j=0}^{\infty} \hat{N}_{jn} (n_j + 1/2) \hbar\omega_j + \sum_{n_k=0}^{\infty} \hat{N}_{kn} (n_k + 1/2) \hbar\omega_k. \quad (10)$$

Here $\hat{N}_{jn} = \hat{c}_{jn}^\dagger \hat{c}_{jn}$ and $\hat{N}_{kn} = \hat{c}_{kn}^\dagger \hat{c}_{kn}$.

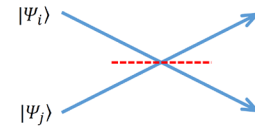


Fig. 3. Two beams of light incident on a beam splitter.

The effects of the beam splitter coupling can be described by an interaction potential $U'(x_j, x_k) = \varepsilon x_j x_k$ where ε is a real constant. Using the definition of the quadratures in Eq. (1), it can be seen that $U'(x_j, x_k)$ will involve $\hat{a}_j^\dagger \hat{a}_k$ and $\hat{a}_k^\dagger \hat{a}_j$, which can transfer photons from one mode to the other. The interaction Hamiltonian \hat{H}' can be written in terms of the field operators as [1]

$$\begin{aligned}\hat{H}' &= \iint dx_j dx_k \hat{\psi}_j^\dagger(x_j) \hat{\psi}_k^\dagger(x_k) \\ &\quad \times U'(x_j, x_k) \hat{\psi}_k(x_k) \hat{\psi}_j(x_j).\end{aligned}\quad (11)$$

A continuous coupling of this kind occurs in two nearby wave guides due to their evanescent fields, for example, which is equivalent to a beam splitter.

In the Heisenberg picture, the time dependence of the operator $\hat{c}_{jn}(t)$ is given by

$$\frac{d\hat{c}_{jn}(t)}{dt} = \frac{1}{i\hbar} [\hat{c}_{jn}(t), \hat{H}], \quad (12)$$

with $\hat{H} = \hat{H}_0 + \hat{H}'$. The commutator in Eq. (12) can be evaluated using Eqs. (3), (9), (10), and (11) combined with the identity

$$\int_{-\infty}^{\infty} \phi_n^*(x) x \phi_n(x) dx = \frac{1}{\sqrt{2}} (\sqrt{n} \delta_{n,n-1} + \sqrt{n+1} \delta_{n,n+1}). \quad (13)$$

This gives

$$\begin{aligned} i\hbar \frac{d\hat{c}_{jn}(t)}{dt} &= \left(n_j + \frac{1}{2} \right) \hbar \omega_j \hat{c}_{jn} \\ &+ \frac{\varepsilon}{2} \sqrt{n} \hat{c}_{j,n-1} \sum_{m=1}^{\infty} \sqrt{m} \hat{c}_{k,m-1}^\dagger \hat{c}_{km} \\ &+ \frac{\varepsilon}{2} \sqrt{n+1} \hat{c}_{j,n+1} \sum_{m=0}^{\infty} \sqrt{m+1} \hat{c}_{k,m+1}^\dagger \hat{c}_{km}. \end{aligned} \quad (14)$$

Two additional terms in Eq. (14) that do not conserve energy have been neglected in the usual rotating-wave approximation [8,20]. The time rate of change of $\hat{c}_{kn}(t)$ is given by a similar expression. This set of coupled equations can be solved to find the form of these operators and their adjoints as a function of time in the Heisenberg picture. The results can then be inserted into Eq. (9) to obtain the form of the field operator.

Eq. (14) and the corresponding equation for $\hat{c}_{kn}(t)$ were solved numerically using the hyperphoton number states $|\dots, N_{jn}, \dots, N_{j0}\rangle \otimes |\dots, N_{kn}, \dots, N_{k0}\rangle$ as a basis for a matrix representation [41]. Given the order of the operators in Eq. (14), it is only necessary to include the states with N_j and N_k equal to 0 or 1 (the initial state corresponds to $N_j = N_k = 1$). We will denote the state with no oscillators in mode j by $|Z_j\rangle = |\dots, 0_{jn}, \dots, 0_{j0}\rangle$, with a similar expression for mode k . The relevant Hilbert subspace for this example includes $|Z_j\rangle$ and $|Z_k\rangle$ in addition to the usual Fock states, and it is only slightly larger than the Hilbert space for conventional quantum optics.

Fig. 4(a) shows the calculated probability density $P(x_j, t) = \langle \hat{\psi}_j^\dagger(x_j, t) \hat{\psi}_j(x_j, t) \rangle$ as a function of time for the case in which the initial state in mode j was a coherent state [8-11] with a mean photon number of $\bar{n}_j = 4$. Mode k was assumed to initially be in its vacuum state $|0_k\rangle$ with no photons. It can be seen that the probability density in mode j is described by a Gaussian distribution whose mean displacement oscillates sinusoidally with a decreasing amplitude. Fig. 4(b) shows the corresponding results for mode k , whose amplitude increases at the expense of mode j due to the beam splitter coupling [42].

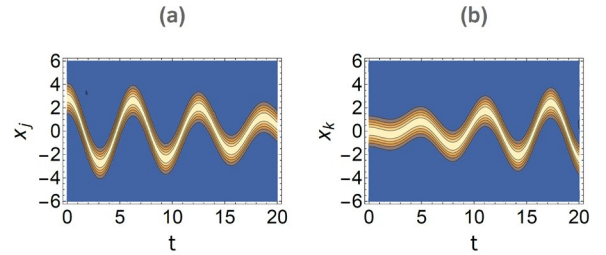


Fig. 4. Effects of a beam splitter on a coherent state incident in mode j with mode k initially in its vacuum state. (a) Probability density $P(x_j, t) = \langle \hat{\psi}_j^\dagger(x_j, t) \hat{\psi}_j(x_j, t) \rangle$ for mode j plotted as a function of the quadrature x_j and the time t . (b) Probability density $P(x_k, t)$ for mode k . The width of these probability distributions is due to vacuum fluctuations. (Arbitrary units.)

One of the advantages of using the third-quantized Heisenberg picture is that $\hat{\psi}_j(t)$ and $\hat{\psi}_k(t)$ only need to be calculated once, after which they can be used with any initial state or measurement. A more interesting example corresponds to the case in which the initial state in mode j is assumed to be a Schrodinger cat state given by

$$|\Psi_j\rangle = c_n (|\alpha\rangle + e^{i\theta} |-\alpha\rangle). \quad (15)$$

Here $c_n \approx 1/\sqrt{2}$ is a normalization constant, $|\alpha\rangle$ is a coherent state with a real amplitude α , and θ is an arbitrary phase shift. Mode k was assumed to initially be in its vacuum state once again. The joint probability density $P_j(x_j, x_k, t)$ can be calculated using

$$P_j(x_j, x_k, t) = \langle \hat{\psi}_j^\dagger(x_j, t) \hat{\psi}_k^\dagger(x_k, t) \hat{\psi}_k(x_k, t) \hat{\psi}_j(x_j, t) \rangle. \quad (16)$$

This is plotted in Fig. 5(a) at the initial time and then again at a later time in Fig. 5(b) after the two beams have passed through the beam splitter. The entanglement produced by the beam splitter [12] can be seen from the fact that x_j and x_k become correlated.

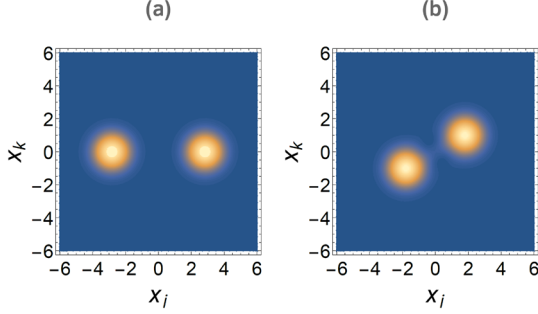


Fig. 5. Joint probability density $P_j(x_j, x_k, t)$ for a Schrodinger cat state plotted as a function of the quadratures x_j and x_k . (a) Joint probability distribution evaluated before the beam splitter ($t=0$). (b) Entangled state produced by the beam splitter [12] with $\varepsilon=0.12$ and $t=12$. (Arbitrary units.)

There are proposed experiments in quantum optics [12,33,37,43] that could measure the expectation value of a coherence operator $\hat{C}_j(x_j, \Delta)$ defined by

$$\hat{C}_j(x_j, \Delta) \equiv \frac{1}{2} [\hat{\psi}_j^\dagger(x_j + \Delta) \hat{\psi}_j(x_j - \Delta)] + h.c. \quad (17)$$

With a suitable choice of the parameter Δ , $\hat{C}_j(0, \Delta)$ can measure the amount of potential quantum interference (coherence) between the two components of the Schrodinger cat state of Eq. (15). This is illustrated in Fig. 6, where $\langle \hat{C}_j(0, \Delta) \rangle$ in the third-quantized Heisenberg picture is plotted as a function of the phase difference θ . The blue (solid) curve shows the interference pattern as measured before the beam splitter, while the red (dashed) curve shows the corresponding results after a beam splitter with the same parameters as in Fig. 5(b). The value of Δ was chosen to maximize the amount of interference in both cases.

Operator $\hat{C}_j(x_j, \Delta)$ measures the coherence of the electromagnetic field between two different points in quadrature space, while earlier coherence functions measure it between different points in space-time [8,20]. In comparison, the coherence operator $\hat{C}_j(x_j, \Delta)$ does not exist in the usual second-quantized Heisenberg approach. As a result, the decoherence

shown in Fig. 6 cannot be calculated in the Heisenberg picture without using the third-quantization approach [41].

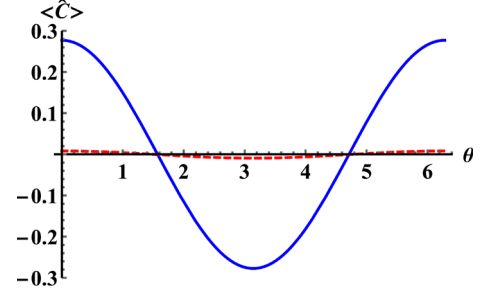


Fig. 6. Quantum interference between the two components of a Schrodinger cat state. The blue (solid) curve shows the expectation value of operator $\hat{C}_j(0, \Delta)$ as a function of θ evaluated before the beam splitter. The red (dashed) curve shows the expectation value of $\hat{C}_j(0, \Delta)$ after the beam splitter using the same parameters as in Fig. 5(b). It can be seen that passing a Schrodinger cat state through a beam splitter will reduce the quantum interference by an amount that is much larger than the reduction in the field amplitude [43]. (Arbitrary units.)

Aside from being a useful computational tool, the third-quantization approach allows an interesting generalization of quantum optics and quantum electrodynamics. The interaction Hamiltonian of Eq. (11) conserves the number of oscillatons and agrees with conventional quantum optics, but in principle there could be other Hamiltonians that do not, such as [41]

$$\hat{H}' = - \int d^3 \mathbf{r} \hat{\mathbf{j}}(\mathbf{r}) \cdot \hat{\mathbf{A}}'(\mathbf{r}). \quad (18)$$

Here $\hat{\mathbf{j}}(\mathbf{r})$ is the second-quantized current associated with another particle, such as an electron, while $\hat{\mathbf{A}}'(\mathbf{r})$ is the vector potential defined in Eqs. (7) and (8) with \hat{c}_{jn} and \hat{c}_{jn}^\dagger replaced using a Bogoliubov transformation [14-17,41,44-48] given by

$$\begin{aligned} \hat{c}_{jn} &\rightarrow \hat{c}'_{jn} = \beta (\cos \gamma \hat{c}_{jn} + \sin \gamma \hat{c}_{jn}^\dagger) \\ \hat{c}_{jn}^\dagger &\rightarrow \hat{c}'_{jn}{}^\dagger = \beta (\sin \gamma \hat{c}_{jn} + \cos \gamma \hat{c}_{jn}^\dagger). \end{aligned} \quad (19)$$

The constant $\beta = 1/(\cos^2 \gamma - \sin^2 \gamma)^{1/2}$ maintains the commutation relations while γ is an unknown angle similar to a mixing angle [41,49-51]. \hat{H}' can create or annihilate pairs of oscillatons if $\gamma \neq 0$, while it reduces to the standard interaction Hamiltonian in the Coulomb gauge [18] for $\gamma=0$. Eq. (18) can also be written in a covariant form in the Lorentz gauge [18].

Experiments could be performed to place an upper bound on γ for various particles interacting with the electromagnetic field, since the existence of oscillatons would be expected to increase the decay rate of excited atoms or more exotic systems such as muonium. Oscillatons could conceivably play a role in the discrepancy observed in recent measurements of the fine structure of positronium [52,53], for example, since Eqs. (18) and (19) would contribute additional Feynman diagrams. These topics require further investigation and are beyond the intended scope of this paper. Some additional comments can be found in the online supplemental material [41].

In summary, a third quantization approach has been introduced in which the usual wave function $\psi_j(x_j)$ for each mode j of the second-quantized electromagnetic field is further quantized to produce a field operator $\hat{\psi}_j(x_j)$. The theory is equivalent to conventional quantum optics and quantum electrodynamics for the case of a single oscillaton per mode ($\gamma = 0$). This approach allows a wide range of phenomena to be analyzed in the Heisenberg picture, including coherence operators, quantum interference, and postselection in quadrature space. Aside from being a useful computational tool, the third quantization of the electromagnetic field allows an interesting generalization of quantum optics and quantum electrodynamics that could be tested experimentally.

Acknowledgements

This work was supported in part by the National Science Foundation under grant number PHY-1802472.

References

1. G. Baym, *Lectures on Quantum Mechanics* (Benjamin, Reading, 1969).
2. L. Schiff, *Quantum Mechanics* (McGraw-Hill, New York, 1955).
3. J.J. Sakurai and J. Napolitano, *Modern Quantum Mechanics*, 2nd ed. (Cambridge University Press, Cambridge, 2017).
4. B.R. Desai, *Quantum Mechanics with Basic Field Theory* (Cambridge U. Press, Cambridge, 2010).
5. R.H. Landau, *Quantum Mechanics II*, 2nd ed. (Wiley, New York, 1996).
6. P. Roman, *Advanced Quantum Theory* (Addison-Wesley, Reading, 1965).
7. E. Koch, in *Emergent Phenomena in Correlated Matter*, E. Pavarini, E. Koch, and U Schollwock, eds. (Institute for Advanced Simulation, Julich, 2013).
8. G.S. Agarwal, *Quantum Optics* (Cambridge U. Press, Cambridge, 2013), p. 7.
9. S.M. Barnett and P.M. Radmore, *Methods in Theoretical Quantum Optics* (Oxford U. Press, Oxford, 1997), p. 64.
10. U. Leonhardt, *Measuring the Quantum State of Light* (Cambridge U. Press, Cambridge, 1997), p. 20.
11. W. Schleich, *Quantum Optics in Phase Space* (Wiley, Berlin, 2001), p. 308.
12. S.U. Shringarpure and J.D. Franson, Phys. Rev. A **102**, 023719 (2020).
13. W.A. Harrison, *Solid State Theory* (McGraw-Hill, New York, 1970).
14. S.M. Girvin and K. Yang, *Modern Condensed Matter Theory* (Cambridge U. Press, Cambridge, 2019).
15. M. El-Batanouny, *Advanced Quantum Condensed Matter Physics: One-Body, Many-Body, and Topological Perspectives* (Cambridge U. Press, Cambridge, 2020).
16. J.R. Schrieffer, *Theory of Superconductivity* (W.A. Benjamin, Reading, 1964).
17. R.D. Parks, ed., *Superconductivity*, Vols. I and II (Marcel Dekker, New York, 1969).
18. C. Cohen-Tannoudji, J. Dupont-Roc, and G. Grynberg, *Photons and Atoms: Introduction to Quantum Electrodynamics* (Wiley, New York, 1989).
19. W. Heitler, *The Quantum Theory of Radiation*, 3rd ed. (Dover, Mineola, 2010).
20. M.O. Scully and M. S. Zubairy, *Quantum Optics* (Cambridge U. Press, Cambridge, 1997).
21. Y. Nambu, Prog. Theor. Phys. **4**, 331 (1949).
22. M. McGuigan, Phys. Rev. D **38**, 3031 (1988).
23. A. Strominger, Phil. Trans. R. Soc. Lond. A **329**, 395 (1989).
24. Y. Xiang and L. Liu, Chin. Phys. Lett. **8**, 52 (1991).
25. Y. Peleg, Class. Quantum Grav. **8**, 827 (1991).
26. T. Prosen, New J. Phys. **10**, 043026 (2008).
27. L.A. Urena-Lopez, Class. Quantum Grav. **19**, 2617 (2002).
28. M.P. Hertzberg, Phys. Rev. D **82**, 045022 (2010).
29. G. Fodor, P. Forgacs, and M. Mezei, Phys. Rev. D **81**, 064029 (2010).
30. M.J. Collett, R. Loudon, and C.W. Gardiner, J. Mod. Optics **34**, 881 (1987).
31. C.M. Caves, Phys. Rev. D **23**, 1693 (1981).
32. D.F. Walls, Nature **306**, 141 (1983).
33. B.T. Kirby and J.D. Franson, Phys. Rev. A **87**, 053822 (2013).
34. S. Stenholm, Physica Scripta **T12**, 56 (1986).
35. A.A. Clerk, M.H. Devoret, S.M. Girvin, F. Marquardt, and R.J. Schoelkopf, Rev. Mod. Phys. **82**, 1155 (2010).
36. C.M. Caves, J. Combes, Z. Jiang, and S. Pandey, Phys. Rev. A **86**, 063802 (2012).

37. J.D. Franson and R.A. Brewster, Phys. Lett. A **382**, 887 (2018).
38. S. Weinberg, Phys. Rev. Lett. **13**, 495 (1964).
39. T.G. Rizzo, Phys. Rev. D **34**, 3519 (1986).
40. M. Suzuki, Phys. Rev. Lett. **56**, 1339 (1986).
41. Additional details can be found in the online supplemental material.
42. W. Schleich, op. cit., p. 307.
43. J.D. Franson and R.A. Brewster, arXiv.1811.06517 (2018).
44. N.N. Bogoliubov, Il Nuovo Cimento **7**, 794 (1958).
45. J.G. Valatin, Il Nuovo Cimento **7**, 843 (1958).
46. C. Emary and R.F. Bishop, J. Math. Phys. **43**, 3916 (2002).
47. A.I. Lvovsky, W. Wasilewski, and K. Banaszek, J. Mod. Opt. **54**, 721 (2007).
48. W.G. Unruh, Phys. Rev. D **14**, 870 (1976).
49. N. Cabibbo, Phys. Rev. Lett. **10**, 531 (1963).
50. S. Weinberg, Phys. Rev. Lett. **19**, 1264 (1967).
51. D. Griffiths, *Introduction to Elementary Particles* (Wiley, Weinheim, 2008).
52. L. Gurung et al., Phys. Rev Lett. **125**, 073002 (2020).
53. M. Rini, Physics **13**, s99, doi.org/10.1103/Physics.13.s99 (2020).

Supplemental Material

Bogoliubov transformation

The Bogoliubov transformation of Eq. (19) was motivated by phenomena in quantum optics [47], superconductivity [16,17], and general relativity [48]. A Bogoliubov transformation can often be used to diagonalize a Hamiltonian, and Eq. (19) can be viewed as a phenomenological description of the effects of an interaction between the oscillators and another hypothetical particle. The bare oscillators would no longer correspond to the true eigenstates of the system as a result of the interaction.

The angle γ is somewhat analogous to a mixing angle, such as the Cabibbo angle [49] or the Weinberg angle [50]. If the hypothetical particle that interacts with the oscillators actually exists ($\gamma \neq 0$), it would be responsible for breaking the symmetry that would otherwise conserve the number of oscillators.

The interaction Hamiltonian of Eqs. (18) and (19) is only one example of possible departures from conventional quantum optics and quantum electrodynamics. For example, there could be a direct coupling between the current and the field operator $\hat{\psi}_j(x_j)$ or its gradient. In addition, the effects of a nonzero oscillator mass could be included in Eq. (10), which assumes that the mass is either zero or negligible. Arbitrary phase shifts could be inserted into the Bogoliubov transformation, and a more general Bogoliubov transformation could couple oscillators in different modes. Eq. (19) appears to be the simplest generalization of quantum optics and quantum electrodynamics based on third quantization, and therefore the most likely.

This paper was originally motivated by the limitations in describing the decoherence produced by beam splitters [43] or optical amplifiers [37] using the second-quantized Heisenberg picture. The author was unaware of the apparent discrepancy between theory and experiment in the positronium experiment of Refs. [52] and [53] until after the first draft of the paper had been written, which included Eq. (19). The third-quantization approach could conceivably play a role in the observed discrepancies, since Eqs. (18) and (19) would contribute additional Feynman diagrams to QED calculations of that kind. Whether or not there is any evidence for the existence of oscillators ($\gamma \neq 0$) remains to be seen. Precision measurements of the magnetic moment of the electron may set the tightest bound on the value of γ .

Terminology

If there were only a single mode of the electromagnetic field, the procedure described in the text would be equivalent to the usual second-quantization formalism. Given that there are an infinite number of modes in the field, the third-quantization approach can be described as a first quantization to obtain the modes, followed by the usual first and second quantization of each of the harmonic oscillators that represent the modes. Third quantization appears to be the simplest way to describe that approach.

One might ask whether or not the oscillators described in the text can be considered to be particles. Texts on quantum optics [8,18] show that the modes of the electromagnetic field are equivalent to harmonic oscillators with no mention of any particle that is actually oscillating. The photons are simply the quantized excitations of the electromagnetic field.

Some insight into this question can be found by noting that the state $|Z_j\rangle$ corresponds to the absence of the usual electromagnetic field. Operator $\hat{\psi}_j^\dagger(x_j)$ acting on $|Z_j\rangle$ creates the usual electromagnetic field in mode j . Acting a second time with operator $\hat{\psi}_j^\dagger(x_j)$ would create a different electromagnetic field with more complicated properties. Thus the oscillators can be viewed as the fundamental components of the electromagnetic field itself. At the same time, the oscillators are the quantized excitations of a hypothetical field and they can be considered to be particles, or perhaps generalized particles, as a result. Somewhat similar issues have been discussed independently in the context of general relativity [22,24].

If experiments show that $\gamma = 0$, then the third-quantization approach would be nothing more than a useful computational tool and these issues of terminology and interpretation would become irrelevant.

Decoherence and the need for the third-quantization approach

One might question the need for the third-quantization approach in analyzing the decoherence produced by a beam splitter in the Heisenberg picture, since the time evolution of an optical system is very simple under a beam splitter transformation. But an analysis of the properties of the system also depends on our ability to define the relevant operators that describe the results of possible experimental measurements. For example, the coherence operator

$\hat{C}_j(x_j, \Delta)$ defined in Eq. (17) does not exist in the conventional Heisenberg picture. As a result, the decoherence of a Schrodinger cat state produced by a beam splitter, as plotted in Fig. 6, cannot be calculated in the usual second-quantized Heisenberg picture [43].

This situation can be understood intuitively from the fact that, in the Schrodinger picture, the wave function $\psi(x)$ gives the probability amplitude that a homodyne measurement will result in that particular value of the quadrature. What gives the probability amplitude of obtaining a particular value of x from a homodyne measurement in the Heisenberg picture? Only the third-quantized field operator $\hat{\psi}(x, t)$ can do that, not the operator $\hat{x}(t)$. As a result, there are experiments in quantum optics that cannot be analyzed in the usual second-quantized Heisenberg picture. This limitation on the use of the conventional Heisenberg picture [37,43] does not appear to be widely appreciated.

An important example of this is the quantum noise produced by a linear optical amplifier, which is commonly analyzed in the Heisenberg picture based on the pioneering work by Caves and others [34-36]. As is well known, the input and output quadrature operators are related by a very simple transformation that is given by

$$\hat{x}_{out} = g\hat{x}_{in} + \hat{N}_{noise}. \quad (20)$$

Here $\hat{x}_{in}(t)$ and $\hat{x}_{out}(t)$ are the input and output quadratures in the usual Heisenberg picture, g is the gain of the amplifier, and \hat{N}_{noise} is a quantum noise operator. There are situations where $g \rightarrow 1$ and $\hat{N}_{noise} \rightarrow 0$ even though there is an exponential decrease in the coherence of a cat state [37]. Eq. (20) would seem to imply that the output field is the same as the input in that case, despite the large decoherence.

This example suggests that the third-quantized field operators $\hat{\psi}_j(x_j, t)$ and $\hat{C}_j(x_j, \Delta, t)$ provide a more complete description of the system than $\hat{x}_j(t)$ does alone, especially for entangled states. Once again, the reason is that the probability amplitude for obtaining a specific value of x from a homodyne measurement can be found from $\hat{\psi}_j(x_j, t)$ but not from the usual operator $\hat{x}_j(t)$. One might attempt to use a Taylor series expansion of $\hat{C}_j(x_j, \Delta, t)$ in powers of $\hat{x}_j(t)^m \hat{p}_j(t)^n$ to calculate the decoherence produced by an optical amplifier in the second-quantized Heisenberg picture, but that does not converge due to the singular nature of $\hat{\psi}_j(x_j, t)$.

As noted earlier in the main text, calculations of this kind could also be performed using the second-quantized Schrodinger picture. One might argue that there is no need to analyze something in the Heisenberg picture if it can be analyzed in the Schrodinger picture instead. But there are many situations where it is simpler to use the Heisenberg picture, or where the Heisenberg picture provides more insight into the situation. Some additional advantages of using the third-quantized Heisenberg picture are discussed below.

Quasiprobability distributions and wave functions

The decoherence effects described in the text can also be calculated in the second-quantized Schrodinger picture using the wave function itself or a quasiprobability distribution. For a single mode j of the electromagnetic field in a pure state, the Wigner distribution is defined as [42]

$$W(x_j, p_j) \equiv \frac{1}{2\pi} \int_{-\infty}^{\infty} dy e^{-ip_j y} \times \psi_j^* \left(x_j - \frac{1}{2} y \right) \psi_j \left(x_j + \frac{1}{2} y \right). \quad (21)$$

The displacement of the wave function by $\pm y/2$ in the Wigner distribution is similar to the displacement by $\pm \Delta$ in Eq. (17) for the operator $\hat{C}_j(x_j, \Delta)$. But the definition of operator $\hat{C}_j(x_j, \Delta)$ does not include the exponential factor involving p_j or the integral that appears in the definition of the Wigner distribution. As a result, $\hat{C}_j(x_j, \Delta)$ is defined in quadrature space rather than phase space. $\hat{C}_j(x_j, \Delta)$ is more closely related to a coherence function than a quasiprobability distribution. It could be normalized in the usual way and higher-order coherence functions can be defined for $N_j > 1$.

A more significant difference between $\hat{C}_j(x_j, \Delta, t)$ and the Wigner distribution can be seen if there are two or more modes that interact, as in the beam splitter example in the text. In that case the third-quantized field operator $\hat{\psi}_j(x_j, t)$ and operator $\hat{C}_j(x_j, \Delta, t)$ include all of the effects of the entanglement with the other mode k , even though they are only a function of one variable. In contrast, the wave function $\psi(x_j, x_k, t)$ would depend on both coordinates and the two-mode Wigner distribution

would be a function of \hat{x}_j , \hat{x}_k , \hat{p}_j , and \hat{p}_k . Eqs. (17) and (21) would have a very different form in that case.

The use of third-quantized field operators may be advantageous compared to using quasiprobability distributions if we need to do a full multi-mode analysis of interacting optical pulses [44]. In that case, there would be an infinite number of interacting modes and the entangled wave function and quasiprobability distributions would all have an infinite number of variables. In contrast, each of the field operators $\hat{\psi}_j(x_j, t)$ would still be a function of only one variable. This situation is somewhat analogous to the use of field operators in solid-state physics, where the density of electrons can be described by a field operator that is a function of only one variable, rather than a wave function with a very large number of variables.

Open systems

The focus here has been on closed systems with unitary transformations. It can be difficult to apply the Heisenberg picture to open systems, where a density matrix or master equation approach may be more appropriate. In principle, the system can always be defined in such a way as to include all of the relevant interactions and maintain unitarity, as was done here to calculate the decoherence of a Schrodinger cat state due to loss. In that sense, the Heisenberg picture could be applied to any situation in quantum optics using the third-quantization approach. This is the case in quantum electrodynamics, for example.

Numerical calculations

Analytic solutions to Eq. (14) would be desirable, but our earlier work [12] on systems of this kind using the Schrodinger picture did not allow analytic solutions in general and that is probably the case for the third-quantization approach as well. Perturbation theory could be used in many other applications of interest, such as quantum electrodynamics, but the interaction is not small in the situation of interest here and perturbation theory cannot be used. As a result, Eq. (14) for $\hat{c}_{jn}(t)$ along with the corresponding equation for $\hat{c}_{kn}(t)$ were solved numerically instead.

The hyperphoton number states $|\dots, N_{jn}, \dots, N_{j0}\rangle \otimes |\dots, N_{kn}, \dots, N_{k0}\rangle$ were used as a basis for a matrix representation of the operators of interest. As discussed in the text, the only relevant states in the examples of interest here correspond to N_j and N_k

equal to 0 or 1, with both values equal to 1 in the initial state.

The mean number of photons in the initial coherent state of mode j was chosen to be $\bar{n}_j = 4$, with the other mode initially in the vacuum state. Since the probability amplitude drops off exponentially with increasing photon number in a coherent state, it was sufficient to cut off the state vector at a maximum number of photons equal to $n_{\max} = 16$ in both modes. The value of n_{\max} was varied to ensure that the cutoff had no significant effect on the results.

With the addition of the state $|Z_j\rangle$ and the usual vacuum state $|0_j\rangle$, the total number of elements in the state vector for mode j alone was equal to $n_{\max} + 2 = 18$. With the same number of elements in mode k , the dimensions of the combined Hilbert space was $(n_{\max} + 2)^2 = 324$. The number of elements in the matrix representation of each of the operators was the square of that, or 104,976. All of the matrices were very sparse and the memory requirements as well as the execution time were greatly reduced using Mathematica's sparse matrix routines.

In order to put the operators in the form of a matrix, it was useful to label each element of the combined state vector with a single index l that ranged from 1 to 324. The way in which the states are labeled is arbitrary, but a suitable choice for the labelling allowed the number of photons in each mode to be written as a simple function of l , for example. That in turn allowed the nonzero values of $\hat{c}_{jn}[l', l, t]$ and $\hat{c}_{kn}[l', l, t]$ to be specified at the initial time $t = t_0$ in a straightforward way using Eq. (6).

The matrices $\hat{c}_{jn}[l', l, t]$ and $\hat{c}_{kn}[l', l, t]$ were then incremented over small time intervals Δt using the fourth-order Runge-Kutta algorithm with derivatives given by Eq. (14). Since the residual errors in the Runge-Kutta algorithm are on the order of Δt^5 , the results converged rapidly and had no significant dependence on the choice of the time step. The results shown in the text were based on the use of 1200 time steps. Built-in Mathematica routines such as NDSolve were not used because they store the results at all of the intermediate steps and require a large amount of memory as a result.

Once $\hat{c}_{jn}[l', l, t]$ and $\hat{c}_{kn}[l', l, t]$ had been calculated, they were inserted into Eq. (9) for the field operator which was then used to calculate the expectation values of interest (using the initial state). The calculations shown in the text required

approximately 10 minutes of computer time and 250 MB of memory on a personal computer.